Precipitation of CuS and ZnS in a Bubble Column Reactor

Mousa Al-Tarazi, A. Bert M. Heesink, and Geert F. Versteeg
Faculty of Science and Technology, University of Twente, Enschede, The Netherlands

Mohammed O. J. Azzam and Khalid Azzam
Chemical Engineering Dept., Jordan University of Science and Technology (JUST), Irbid, Jordan

DOI 10.1002/aic.10310
Published online in Wiley InterScience (www.interscience.wiley.com).

This work presents an experimental study into the precipitation of CuS and ZnS in a semibatch-wise operated bubble column. First the applied bubble column was characterized with respect to mass transfer phenomena. The influences of ionic strength and superficial gas velocity on volumetric mass transfer coefficient and gas holdup, respectively, were determined using both CO_2 and H_2S gas. Increasing the ionic strength was found to increase the gas holdup and volumetric mass-transfer coefficient. Although the gas holdup with H_2S was found to be higher than that with CO_2 at the same ionic strength and superficial gas velocity, the measured volumetric mass transfer coefficient was for CO_2 absorption. In the second part of the study the influences of the H_2S gas concentration, initial metal concentration and gas pressure on the precipitation of ZnS and CuS were investigated. With increasing H_2S concentration, the initial concentration or pressure of Zn ions yields a decrease in the average size of produced ZnS particles. No significant effects could be observed when producing CuS particles. This was probably a result of the surface activity of such particles, causing them to cluster and form agglomerates. The results are useful for scale-up and design of similar types of precipitator.
 AIChE J, 51: 235–246, 2005
Keywords: bubble column, hydrodynamics, precipitation, zinc sulfide, copper sulfide

Introduction

Bubble columns are widely used in industry as gas–liquid (–solid) contactors because of their simple construction and operation.[1] Bubble columns are applied not only for biotechnological or environmental purposes but also for conventional chemical reactions as in the methanol synthesis. The bubble column in its simplest form does not contain sensitive mechanical devices such as stirrers and can be built in various dimensions (see Figure 1).

A bubble column consists of a vertical cylinder containing both liquid and gas dispersed as bubbles. The bubbles either are homogeneous in size (at relatively low superficial gas velocities) or are heterogeneous in size (at high superficial velocities); larger bubbles rise faster than smaller ones.[2] The heterogeneous regime is characterized by intense liquid circulation, turbulence, and large eddies that are nonstationary with respect to time and space.

For the design of a bubble column, knowledge of various design parameters such as mass transfer coefficients, gas holdup, residence time distribution, rate of mixing, and pressure drop is crucial. The prevailing procedures used to quantify these parameters are largely empirical and in most cases experimental work is needed. A more fundamental approach is possible through the understanding of macro- and microflow patterns.[3] Much progress has been achieved, although a general model that is able to simulate all interactions simultaneously is still a distant reality.

Besides a gas and a liquid phase, a solid phase is added or formed inside the bubble column in some industrial applica-

Correspondence concerning this article should be addressed to M. Al-Tarazi at www.utwente.nl.

tions such as the production of (in)organic salts, fine chemicals, and biotechnological materials.[4] The design of a bubble column in which solids are formed is rather complex because many phenomena interact: multiphase flow dynamics, mass transfer, chemical reactions, as well as nucleation and growth of crystals. The ultimate challenge is to predict and control the physical properties of produced solids such as their mean particle size. Although precipitation is a common operation in chemical industry, it remains very difficult to predict the size distribution of the produced particles. Particle size is a complex function of nucleation rate, crystal growth, and agglomeration of the crystals.[5] Therefore determination of the influence of different process conditions on the behavior of a bubble column and product quality is of crucial importance for the design and control of a bubble column precipitator.

In gas–liquid precipitation reactions, a gaseous reactant A is contacted with a liquid solution of reactant B.[6] Gas A is absorbed into the solution, dissociates, and reacts instantaneously with B ions to produce AB clusters. When the concentration of the produced clusters exceeds the solubility concentration, supersaturation occurs. Because of the generated supersaturation, nuclei are formed that start to grow to form crystals. When the concentration of the crystals increases, the chances for forming agglomerates or aggregates become higher. If two or more crystals meet they may aggregate and grow further as one crystal. All steps are illustrated in Figure 2.

Heavy metal ions such as copper and zinc that are present in the wastewater of a zinc factory can be precipitated as copper sulfide and zinc sulfide when contacted with hydrogen sulfide (H_2S).[7,8] This work is part of a large study of the precipitation of heavy metal ions (mainly Cu^{2+} and Zn^{2+}) present in wastewater from the Pasminco zinc factory in Budel, The Netherlands. Use is made of the Paques Thiopaq® process, involving biological reduction of sulfate, which is also present in the wastewater, toward sulfide. The sulfide subsequently reacts with the metal ions to form metal sulfides that can be removed by use of a settler or a centrifuge. To enable sufficient removal of the metal sulfides, coarse particles are to be produced (>10 μm). The size distribution of the solid particles is fully determined by precipitation conditions, which may vary quite significantly from the gas–liquid interface to the liquid bulk. This size distribution is of great importance for separation and downstream processing of the particles. In this work the precipitation of copper sulfide and zinc sulfide in a bubble column reactor is studied to gain a better understanding of the relevance between the process conditions and the formation of CuS and ZnS solids.

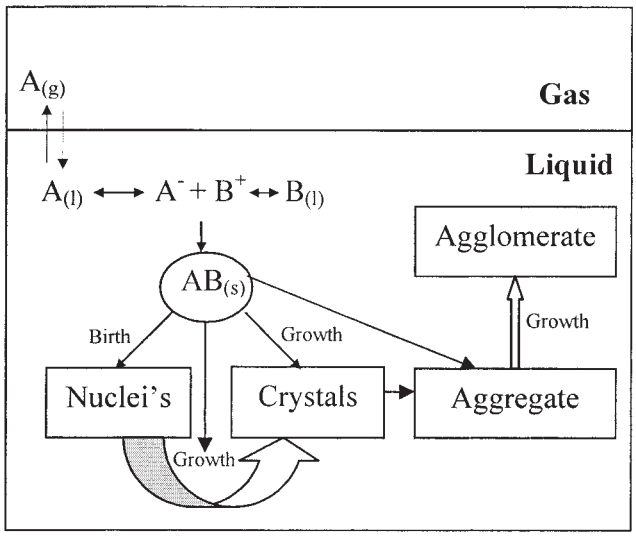

Figure 2. Gas–liquid precipitation reaction.

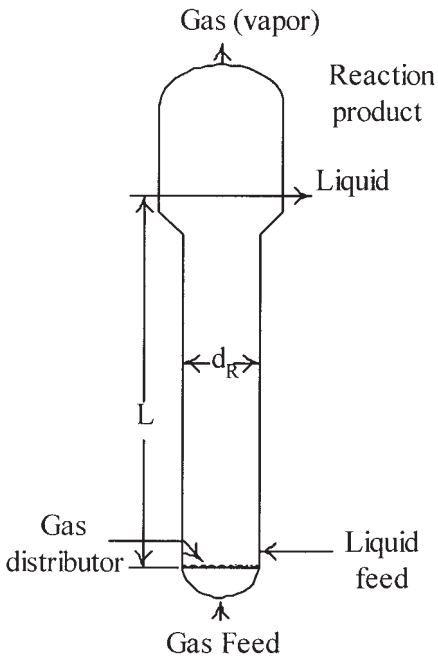

Figure 1. Simple bubble column.

Literature Survey

Marracci[9] developed a theory that describes the effect of the electrolyte concentration on bubble coalescence. According to Marracci, salts inhibit bubble coalescence by retarding the thinning of the intervening liquid film between bubble pairs. Moreover, it was concluded that increasing the salt concentration increases the film surface tension, which develops an opposite force to the direction of the flow at the gas–liquid boundary. As a result of that, the thinning time during bubble coalescence increases. At sufficiently high salt concentrations, this force even immobilizes the gas–liquid interface.

Alvarez-Cuena and Nerenberg[10] used the plug-flow module (PFM) to study mass transfer inside a bubble column and to predict concentration profiles. They aimed to show the significance of the volumetric mass transfer coefficient when using the PFM for design purposes. An analysis of the PFM was made by comparing experimental and calculated concentration profiles over the entire column. Relative deviation, as high as 68%, was observed in the grid region. They concluded that the PFM cannot describe mass transfer in bubble columns.

Wach and Jones[11] studied the characteristics of gas–liquid heterogeneous precipitation systems by measuring particle size distributions under various operating conditions and mass transfer resistances. They used a mixed-suspension, mixed-product removal reactor (MSMPR) in their experiments. They found that the mass transfer resistance affects the average

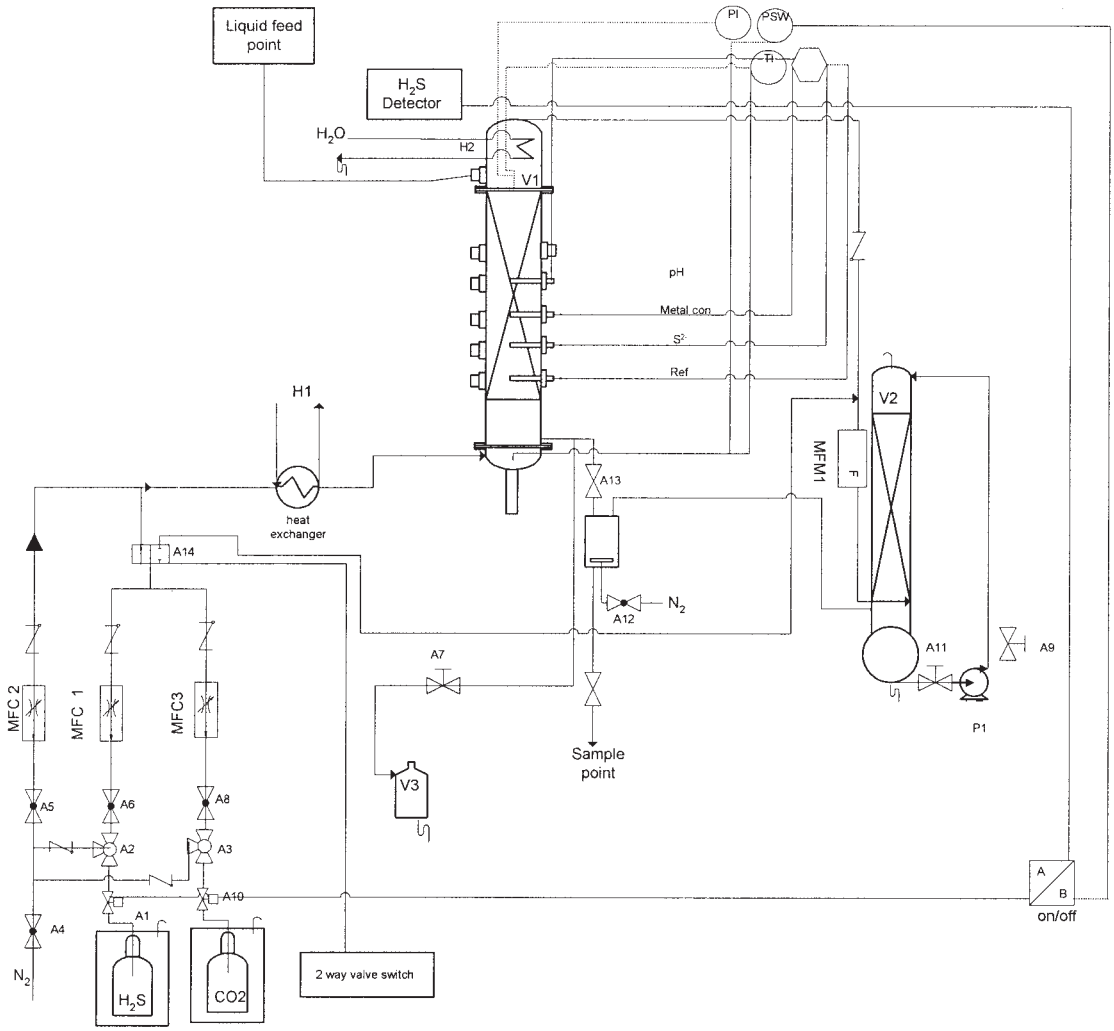

Figure 3. Experimental setup for the precipitation of heavy metals from wastewater.

particle size. Larger particles were formed under conditions of high mass transfer into a large liquid volume (high Hinterland ratio), whereas small particles were produced at low mass transfer coefficients.

Tsutsumi et al.[12] studied the role of bubble wakes in the formation of calcium carbonate particles in a semibatch bubble column reactor. They found that secondary nucleation occurred in the wake region and explained this by the attrition of crystals caused by vortical motion. They also found that during the early stages of reaction a significant change in the size distribution of agglomerates occurs in the wake.

Jones et al.[13] studied the effect of liquid mixing on the average particle size of calcium carbonate particles in a small flat-interface gas–liquid reaction cell. It was found that crystal size increases with increasing agitation rate stemming from its effect on gas–liquid mass transfer.

Deckwer and Schumple[14] presented a review of the correlations available for the estimation of gas holdup, mass transfer, and mixing coefficients. According to them the uncertainties and errors in the bubble column design arise partly from oversimplification in the applied models.

Hostomsky and Jones[15] used the penetration model to describe mass transfer and crystal precipitation near the gas–liquid interface and to predict the effect of liquid agitation on the mean particle size of precipitates while using thermodynamic and kinetic data from literature. It was found that at decreasing mass transfer rate, the nucleation rate increases in the region close to the interface. Nucleation rate, particle number density, and the mean particle size were found to be maximal at a certain distance from the gas–liquid interface.

Eigenberger and Bauer[3] developed a concept for iterative multiscale modeling and simulation of gas/liquid bubble column reactors with and without liquid recycling. Their concept includes mass transfer accompanied by chemical reaction as well as detailed (unsteady state) hydrodynamics. They used a one-dimensional model to describe mass transfer and reaction rate and coupled that with a hydrodynamic model to predict bubble size and bubble size distribution.

Teixeira et al.[7] studied the effect of orifice diameter in the distributor plate, airflow rate, solid loading, and solid density on hydrodynamics (gas holdup, circulation time, and liquid velocity) of a three-phase external-loop airlift reactor. They observed that the gas distributor has a negligible effect on gas holdup, circulation time, and downcomer liquid velocity. How-

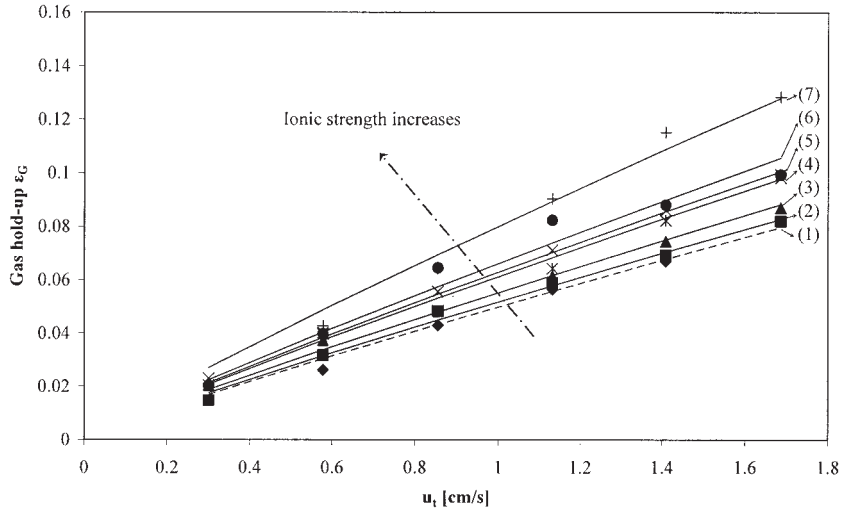

Figure 4. Effects of superficial gas velocity and ionic strength on gas holdup (ε_G).

Conditions: T = 20°C, V_L = 2 L, P = 1.01 bar, gas = CO_2. Ionic strength (in M): (1) 0.025; (2) 0.05; (3) 0.1; (4) 0.25; (5) 0.5; (6) 1.0; (7) 2.0.

ever, airflow rate, solid loading, and solid density appeared to produce significant effects.

Jones and Rigopoulos[4] presented a dynamic model of a bubble column reactor with particle formation, using a hybrid computational fluid dynamics (CFD)–reaction engineering approach. They used CFD for estimating the hydrodynamics based on the two-phase Eulerian–Eulerian method. They made use of the penetration theory as well as the population balance to predict average particle size. They applied the model on the precipitation of $CaCO_3$ by CO_2 absorption into a $Ca(OH)_2$ solution in a draft tube bubble column and obtained insight into phenomena underlying crystal size evolution.

Joshi[2] presented an article that reviews the modeling efforts on bubble column flow patterns of the last 30 years. According to his review developments mainly were on three fronts: (1) formation of interface forces, (2) closure problem for the eddy viscosity, and (3) modeling of the Reynolds averaging procedure.

Kluytmans et al.[16] studied the effects of electrolyte and particle concentrations on the gas holdup in a slurry bubble column for both the homogeneous and the heterogeneous flow regime. They determined bubble behavior in a 2D slurry column by videorecording, and also measured gas holdup. They found that adding electrolyte or solid carbon particles leads to a substantial increase in gas holdup until a critical concentration is reached. Afterward no further effects were found. According to their results the conditions for transition from the homogeneous to the heterogeneous regime were not influenced by the concentration of the electrolyte or the solid particles.

Bouaifl et al.[17] studied gas holdup, mass transfer, interfacial area, bubble size, and bubble distribution in bubble columns as well as vessels equipped with various dual impellers. They

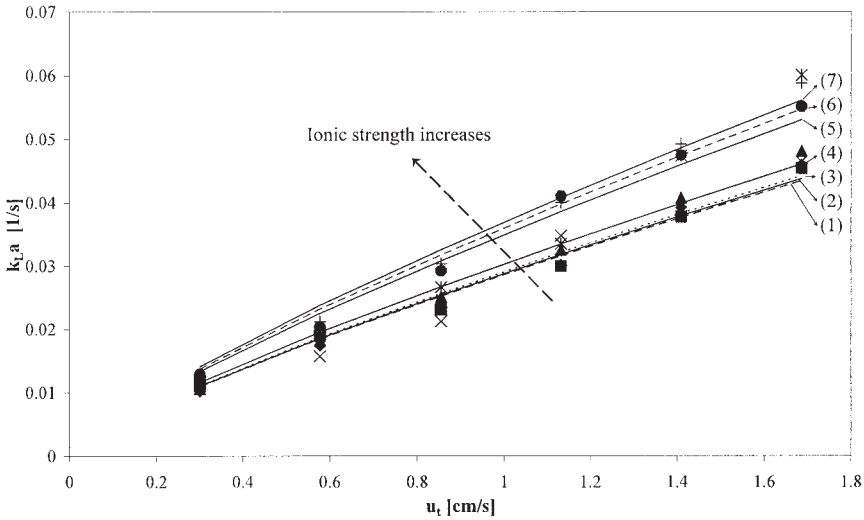

Figure 5. Effects of superficial gas velocity and ionic strength on the volumetric mass-transfer coefficient (k_La).

Conditions: T = 20°C, V_L = 2 L, P = 1.01 bar, gas = CO_2. Ionic strength (in M): (1) 0.025; (2) 0.05; (3) 0.1; (4) 0.25; (5) 0.5; (6) 1.0; (7) 2.0.

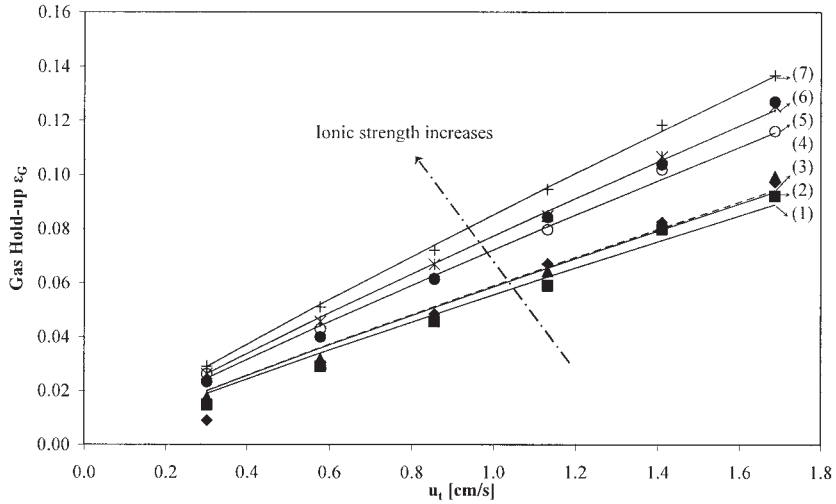

Figure 6. Effects of superficial gas velocity and ionic strength on gas holdup (ε_G).

Conditions: $T = 20°C$, $V_L = 2$ L, $P = 1.01$ bar, gas = H_2S. Ionic strength (in M): (1) 0.025; (2) 0.05; (3) 0.1; (4) 0.25; (5) 0.5; (6) 1.0; (7) 2.0.

studied the effects of gas flow rate, sparger type, and column diameter in bubble column. They compared their results with similar results reported in the literature.

The present work focuses on the precipitation of water-dissolved heavy metals (copper or zinc) by contacting these with hydrogen sulfide gas in a bubble column contactor. Volumetric mass transfer and gas holdup were studied using both CO_2 and H_2S gases. The effects of ionic strength and superficial velocity on mass transfer and gas holdup were investigated as well as the effects of copper/zinc concentration, superficial gas velocity, and H_2S concentrations on the size distribution of the produced metal sulfide particles. The study provides more insight into the precipitation reaction as well as useful correlations for design scale-up processes of such systems.

Experimental

The applied experimental setup is illustrated in Figure 3. The bubble column reactor was a double-walled glass vessel having a length of 60 cm and an internal diameter of 7.5 cm. A cooler was placed at the top of the column to condense any evaporated water. The temperature of the gas feed (N_2/H_2S or N_2/CO_2) and the column was controlled by means of a thermostat bath. All experiments were carried out at 20°C. The flow rate and composition of the gas were controlled with the help of electronic mass flow controllers (MFCs). The flow rate of the effluent gas was measured by using an electronic mass flow meter (MFM). The column was operated under semibatch conditions, implying a continuous gas flow through a single

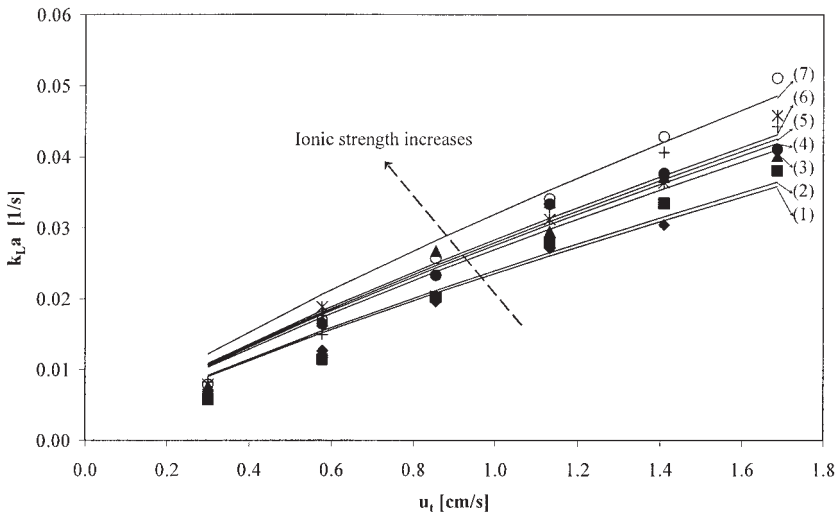

Figure 7. Effects of superficial gas velocity and ionic strength on the volumetric mass transfer coefficient (k_La).

Conditions: $T = 20°C$, $V_L = 2$ L, $P = 1.01$ bar, gas = H_2S. Ionic strength (in M): (1) 0.025; (2) 0.05; (3) 0.1; (4) 0.25; (5) 0.5; (6) 1.0; (7) 2.0.

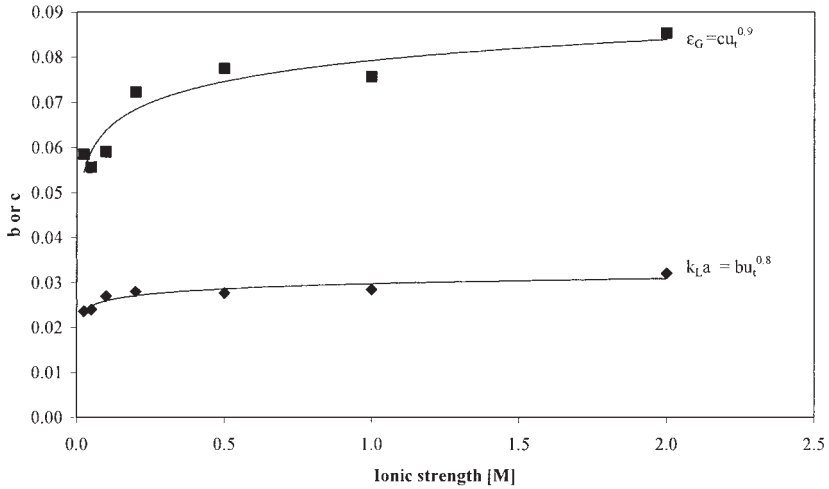

Figure 8. Effects of ionic strength on the fitting parameter *b* or *c* for both volumetric mass transfer coefficient (k_La) and gas holdup (ε_G).

Conditions: T = 20°C, V_L = 2 L, P = 1.01 bar, gas = H_2S.

batch of liquid (demiwater or a solution of $CuSO_4$ or $ZnSO_4$ in demiwater). The effluent was sent to a scrubber to remove any nonabsorbed H_2S. Temperature, pressure, pH, metal concentration (in the case of copper), sulfide concentration, and inlet/outlet gas flow rates were registered every second by a PC. Samples were taken during and after each precipitation experiment for the determination of particle size distribution and metal concentration. Just after sampling, the samples were stripped with N_2 to remove any dissolved H_2S. Particle size was measured by X-ray diffraction (0.1–704 μm, Microtrac X-100) or dynamic light scattering (DLS; 1–5000 nm, Zeitasizer 5000), depending on the size of the produced particles. After a sample was taken from the reactor, a small amount of Triton X-100 was added to prevent particle agglomeration and to fixate the size distribution of the produced particles (0.1 mL of X-100/1000 mL of sample).

This work is divided into two parts: (1) a study of bubble column hydrodynamics and (2) precipitation of zinc and copper sulfide in that same bubble column. All experiments were carried out in the homogeneous bubble regime. The first part involves determination of the gas holdup and the volumetric mass transfer coefficient (k_La) while using pure CO_2 and H_2S gas. The effects of superficial gas velocity as well as ionic strength of the solution were investigated. The volumetric mass transfer coefficient (k_La) was determined by monitoring the concentration of CO_2 or H_2S in the solution as a function of time after starting the gas supply (see Eqs. 1a–1c). Concentrations of CO_2 or H_2S were determined from the mass balance over the gas phase. Gas holdup was calculated from experimentally observed values of the liquid height and the height of the gas–liquid dispersion (see Eq. 2)

$$\frac{dc_A^b}{dt} = k_La(c_A^i - c_A^b) \tag{1a}$$

where A is either CO_2 or H_2S

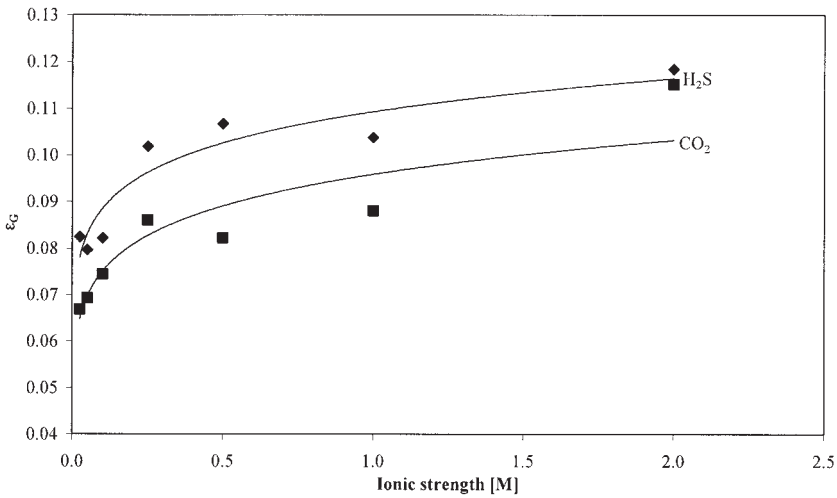

Figure 9. Effects of ionic strength on gas holdup (ε_G) for both CO_2 and H_2S gases.

Conditions: T = 20°C, V_L = 2 L, P = 1.01 bar, u_t = 1.41 cm/s.

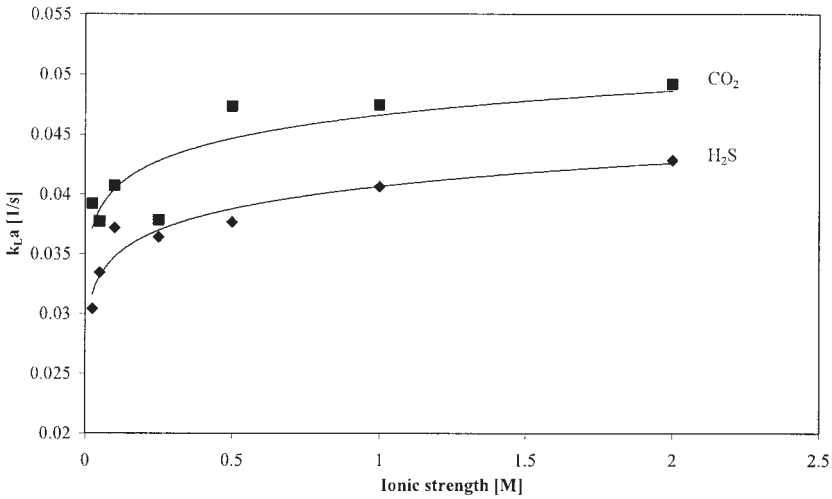

Figure 10. Effects of ionic strength on the volumetric mass-transfer coefficient (k_La) for both CO_2 and H_2S gases.
Conditions: $T = 20°C$, $V_L = 2$ L, $P = 1.01$ bar, $u_t = 1.41$ cm/s.

$$c_A^b = \frac{\dot{m}_{in} - \dot{m}_{out}}{V_L} \tag{1b}$$

$$\ln\left(\frac{c_A^i - c_A^o}{c_A^i - c_A^b}\right) = k_L a t \tag{1c}$$

$$\varepsilon_G = \frac{V_d - V_L}{V_d} \tag{2}$$

The experimentally obtained values of k_La and ε_G were fitted as a function of superficial velocity using simple power-law relationships

$$k_L a = b u_t^{0.8} \tag{3a}$$

$$\varepsilon_G = c u_t^{0.9} \tag{3b}$$

In the second part of the study (precipitation), the bubble column was operated in semibatch mode, whereas a mixture of H_2S and N_2 was used to precipitate the Cu^{+2} or Zn^{+2} ions present in the solution. The ionic strength of the solution was kept constant by adding excess KCl salt. In these experiments, the flow rates of influent and effluent as well as temperature, pressure, and pH were monitored vs. time. At the end of each experiment a sample was taken and analyzed by X-ray (0.45–3000 μm) or DLS (1–5000 nm) to measure the particle size distribution of the formed solids. The metal concentration was measured at the beginning and at the end of each experiment using an atomic absorption spectrometer (AAS). The effects of initial metal concentration, inlet H_2S concentration, and pressure on the average H_2S flux, metal conversion, and average particle size were investigated. The average H_2S flux was calculated using the mass balance on the gas side (see Eq. 4). The specific area of the bubble column was estimated using Eq. 5[20]

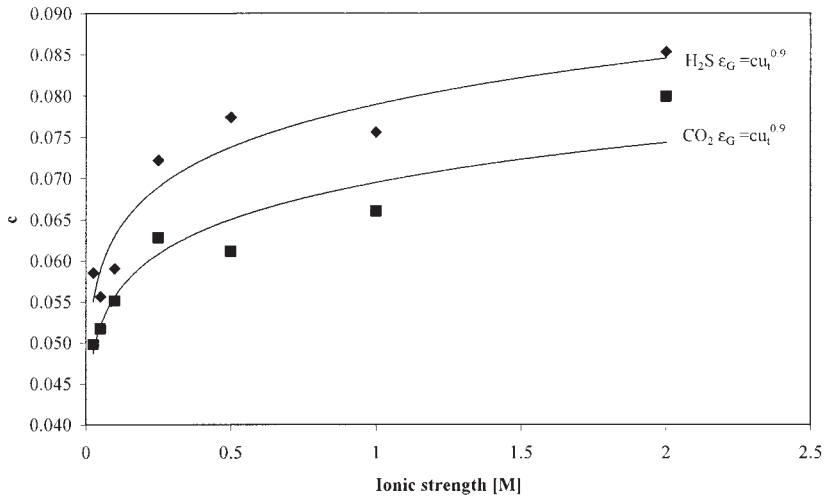

Figure 11. Effects of ionic strength on the fitting parameter c of gas holdup (ε_G) for both CO_2 and H_2S gases.
Conditions: $T = 20°C$, $V_L = 2$ L, $P = 1.01$ bar, $u_t = 1.41$ cm/s.

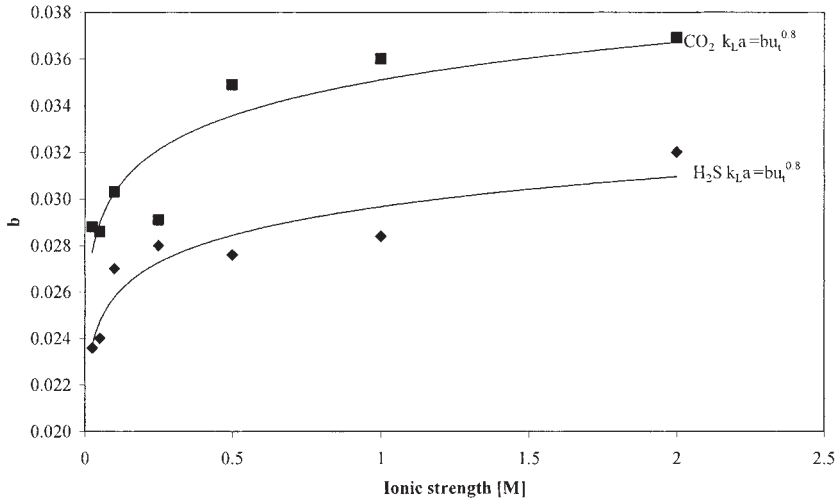

Figure 12. Effect of ionic strength on the fitting parameter *b* for the volumetric mass transfer coefficient (k_La) for both CO_2 and H_2S gases.

Conditions: $T = 20$°C, $V_L = 2$ L, $P = 1.01$ bar, $u_t = 1.41$ cm/s.

$$J_{H_2S} = \frac{\dot{m}_{in} - \dot{m}_{out}}{aV_L}(1 - \varepsilon_G) \tag{4}$$

$$a = 3.32[u_t \rho_L g(1 - \varepsilon_G)]^{0.69} \tag{5}$$

Results and Discussion

The effects of superficial velocity and ionic strength on gas holdup (ε_G) and the volumetric mass transfer coefficient (k_La) when using CO_2 are shown in Figures 4 and 5, respectively. In the figures, the points represent the experimental values and the lines represent the fits according to Eqs. 3a–3b; the exponent n was fixed at 0.9 for ε_G and at 0.8 for k_La. Only the preexponential values of b and c were calculated to obtain the best fit. The best-fit values of b were found to vary from 0.05 to 0.08, whereas those of c varied from 0.029 to 0.037. As expected, values of both ε_G and k_La increase with increasing superficial gas velocity because it increases the bubble population density.[1,18] It is known from the literature that further increasing the superficial velocity will result in bubble coalescence and finally to a constant gas holdup,[17] On the other hand, upon increasing the superficial velocity the mass transfer coefficient k_L will continuously increase as a result of the formation of bigger bubbles that have a higher rise velocity,[1,2,6,20] whereas an increase in average bubble size will correspond with a decrease in interfacial area.[20] However, the overall effect of increasing the gas velocity on volumetric mass transfer coefficient was always positive.

Increasing the ionic strength increases the values of both ε_G and k_La. This can be attributed to an increase in surface tension,[19] which stabilizes the bubbles and decreases bubble coalescence.[9]

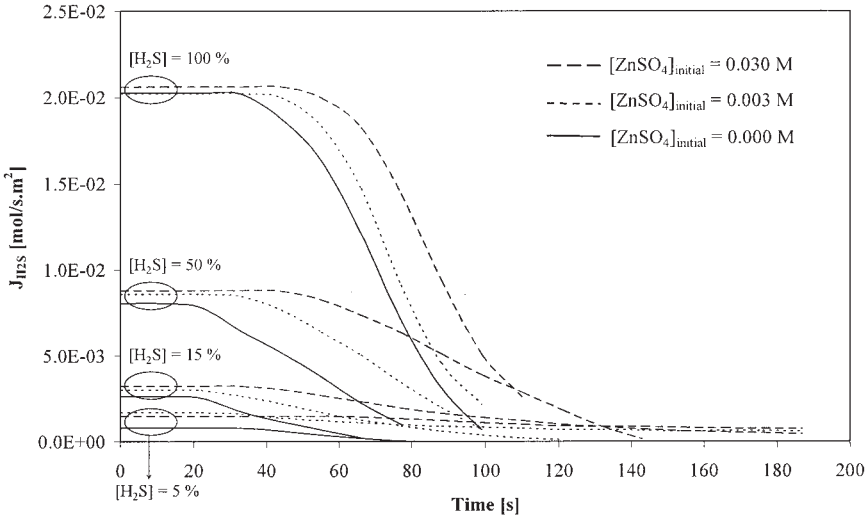

Figure 13. Effect of initial zinc ions concentration and H_2S inlet concentration on average H_2S flux.

Conditions: $T = 20$°C, $V_L = 1.5$ L, $P = 1.27$ bar, $u_t = 2.15$ cm/s, specific area (a) = 89.56 m^2/m^3, $k_La = 0.0524$ 1/s, ionic strength = 1 M.

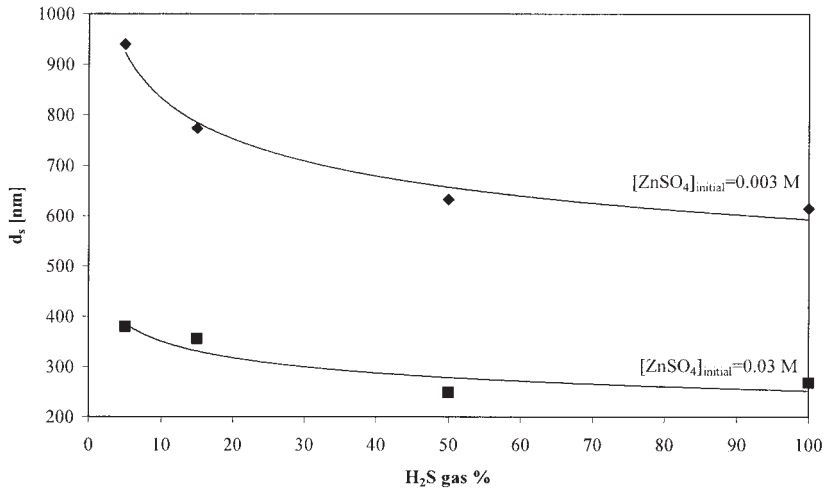

Figure 14. Effect of inlet H_2S concentration on the average particle size of the produced solids.

Conditions: $T = 20°C$, $V_L = 1.5$ L, $P = 1.27$ bar, $u_t = 2.15$ cm/s, specific area (a) = 89.56 m^2/m^3, $k_La = 0.0524$ 1/s, ionic strength = 1 M.

Figures 6, 7, and 8 show the effects of superficial velocity and ionic strength on gas holdup and volumetric mass transfer coefficient when using H_2S. In general the same trends were found as with the CO_2 experiments. However, gas holdup values were higher for H_2S than for CO_2 (see Figures 9 and 11). This can arise from a difference between the surface tensions of the water–CO_2 and water–H_2S. On the other hand the measured k_La values for H_2S were lower than those for CO_2 (see Figures 10 and 12). This is mainly attributed to the formation of smaller bubbles when H_2S is used (observed experimentally) that rise more slowly. In general the values of k_La and ε_G increased with ionic strength and superficial gas velocity in a power-law manner. The most significant influence was observed at low ionic strengths and low superficial velocities.

Figure 13 shows the effects of H_2S inlet concentration and initial zinc ions concentration on the average H_2S flux. The first parts of the curve represent the displacement of nitrogen that already exists in the gas cap of the bubble column as well as the reaction with metal ions (if present). After most metal ions have been consumed and the nitrogen is displaced, the H_2S concentration in the liquid starts to increase. Because of this increase in H_2S concentration the overall driving force starts to decrease and, consequently, the H_2S flux starts to decrease as well. In a comparison of the natural absorption curve (without metal ions) with reaction curves, three important differences can be noticed: (1) it takes more time for a reactive system to build up H_2S in the liquid, (2) there is a small chemical enhancement of mass transfer arising from the fast precipitation reaction,[21] and (3) some enhancement still occurs even after the reaction has been completed.[1,18,20] Chemical enhancement increases with the concentration of zinc ions, as expected.[21] Chemical enhancement stems from the fact that the reaction between S^{2-} and Zn^{2+} is instantaneous. The infinite enhancement factor can be calculated from

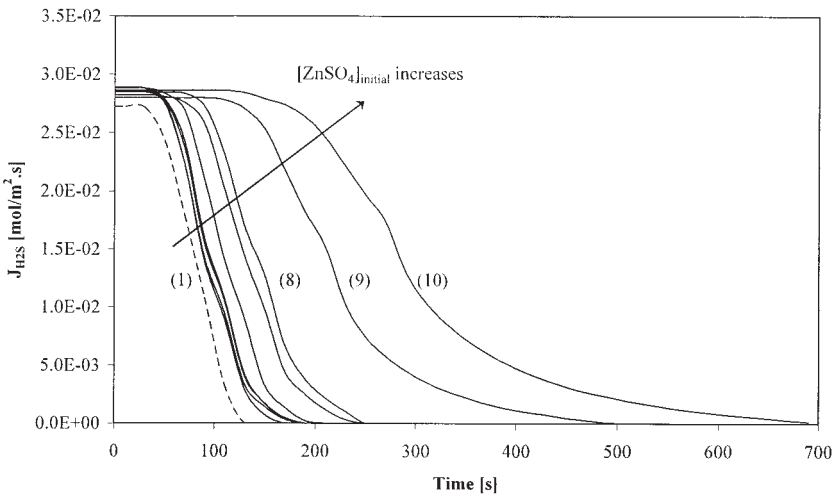

Figure 15. Effect of initial $ZnSO_4$ concentration on the H_2S flux.

Conditions: $T = 20°C$, $V_L = 1.5$ L, $P = 1.36$ bar, $u_t = 1.41$ cm/s, specific area (a) = 69.79 m^2/m^3, $k_La = 0.0406$ 1/s, ionic strength = 1 M, H_2S inlet concentration = 100%, $X = 50–60\%$. Initial $ZnSO_4$ concentration (in M) (1) 0.0; (2) 0.001; (3) 0.003; (4) 0.007; (5) 0.01; (6) 0.03; (7) 0.08; (8) 0.1; (9) 0.3; (10) 0.5.

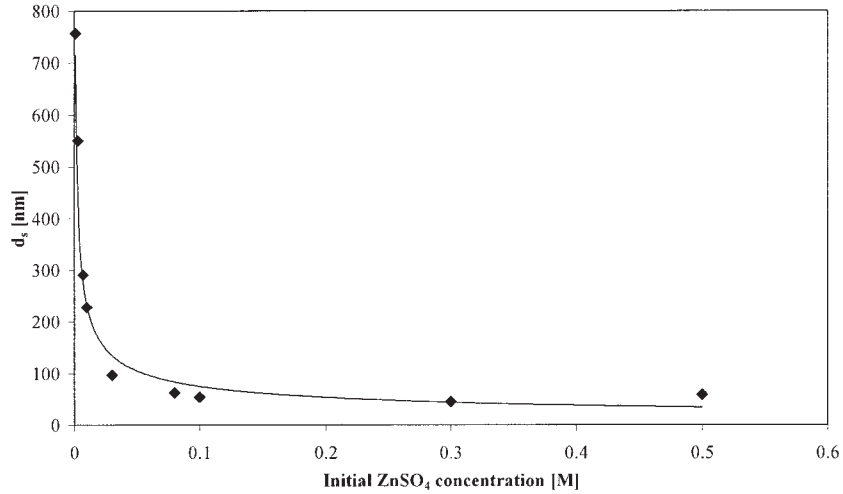

Figure 16. Effect of the initial $ZnSO_4$ concentration on the average particle size.

Conditions: $T = 20°C$, $V_L = 1.5$ L, $P = 1.36$ bar, $u_t = 1.41$ cm/s, specific area (a) = 69.79 m^2/m^3, $k_La = 0.0406$ 1/s, ionic strength = 1 M, H_2S inlet concentration = 100%, $X = 50–60\%$.

$$E_{A,\infty} \cong 1 + \frac{D_{Zn^{2+}}\bar{c}_{Zn^{2+}}}{\nu_{Zn^{2+}}D_{H_2S}c^i_{H_2S}}\left(\frac{D_{H_2S}}{D_{Zn^{2+}}}\right)^{0.5} \tag{6}$$

The obtained values are only slightly higher than unity, which is in agreement with the small enhancement that is initially observed.

Figure 14 shows the effect of the H_2S inlet concentration on the average particle size of the produced ZnS at different initial zinc concentrations. Increasing the H_2S inlet concentration will decrease the average particle size of the produced solids because (local) supersaturation will increase and thus the rate of nucleation as well.[11] Increasing the concentration of zinc ions has a similar effect. See Figures 15 and 16, which show the effects of initial zinc ions concentration on the average H_2S flux and the average size of the produced particles. In general, increasing the initial metal concentration corresponds with an increase in H_2S flux and a decrease of the average size of the produced solids. An increase of the metal concentration will lead to steeper concentration profiles near the interface, and therefore higher H_2S fluxes.[21] Good agreement was found between the measured enhancement factor and the calculated values, assuming instantaneous reaction (Eq. 6). The gas holdup was also observed to increase with increasing initial zinc concentration. This can be explained by the fact that solids attach to the bubbles, thereby stabilizing the bubbles and decreasing bubble coalescence.[18] On the other hand, attached solids cause the bubbles to slow down and reduce the available gas–liquid interface. Finally, the solids can act as transport accelerators by adsorbing H_2S at the interface and carrying it to the liquid bulk. The net effect of all phenomena together apparently was positive because enhancement was experimentally observed.

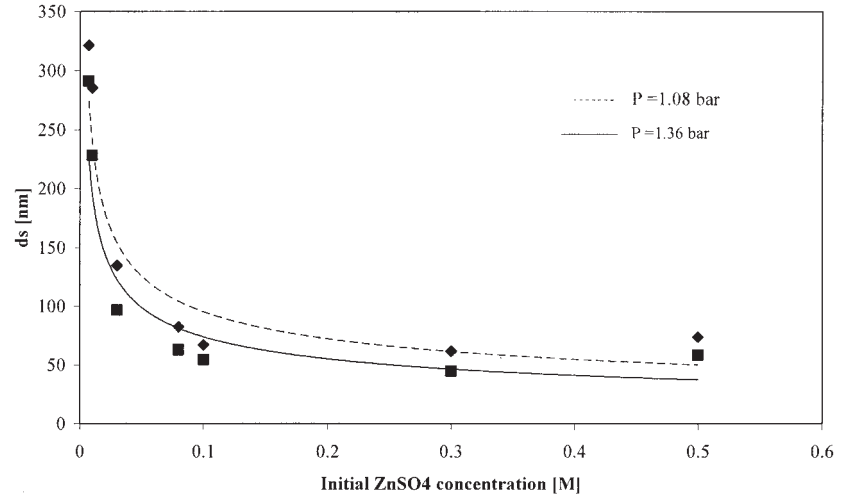

Figure 17. Effects of bubble column pressure and initial $ZnSO_4$ concentration on the average particle size.

Conditions: $T = 20°C$, $V_L = 1.5$ L, $u_t = 1.41$ cm/s, specific area (a) = 69.79 m^2/m^3, $k_La = 0.0406$ 1/s, ionic strength = 1 M, H_2S inlet concentration = 100%, $X = 50–60\%$.

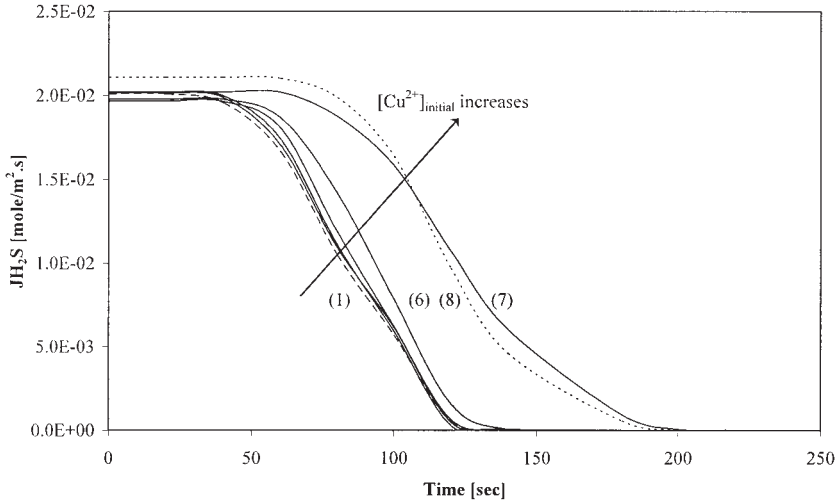

Figure 18. Effect of copper ions concentration on the average flux of H_2S.

Conditions: $T = 20°C$, $V_L = 1.5$ L, $P = 1.01$ bar, $u_t = 1.41$ cm/s, H_2S gas concentration = 100%. Initial $CuSO_4$ concentration (in M): (1) 0.001; (2) 0.003; (3) 0.007; (4) 0.01; (5) 0.03; (6) 0.08; (7) 0.1.

The effect of gas pressure on the average particle size is shown in Figure 17. Increasing the bubble column pressure by 0.3 bar leads to a decrease of the average particle size of about 25%. Increasing the system pressure corresponds with an increase in gas concentration and, consequently, with a higher H_2S concentration on the liquid side. This increase in H_2S concentration increases the supersaturation and thus the nucleation rate and the growth rate of the crystals.[11,13,15] However, a higher supersaturation is more favorable for primary nucleation than for crystal growth and thus more particles of smaller size are produced.[13]

Precipitation experiments were carried out with copper ions as well. Figures 18 and 19 show the effects of the copper ion concentration on the average H_2S flux and the average size of the produced CuS particles. A slight increase in average H_2S flux was observed with increasing initial copper ion concentration. Because the applied concentrations were quite low, hardly any enhancement in H_2S flux was observed (see Eq. 6). The average size of the produced particles also scarcely varied with the concentration of copper ions. Based on the difference in the solubility products of ZnS and CuS (CuS being much less soluble), much smaller particles were expected when using copper instead of zinc. However, copper sulfide particles were found to be surface active and to cluster at the gas–liquid interface, resulting in the formation of agglomerates. These agglomerates make it very difficult to observe any effect of copper concentration on the average particle size. It must be noted that the agglomerate sizes of CuS are in the order of 10–15 μm, whereas the ZnS particles were maximally about 0.5 μm.

Conclusions

The precipitation of CuS and ZnS by contacting an aqueous solution of $CuSO_4$ or $ZnSO_4$ with H_2S gas in a bubble column

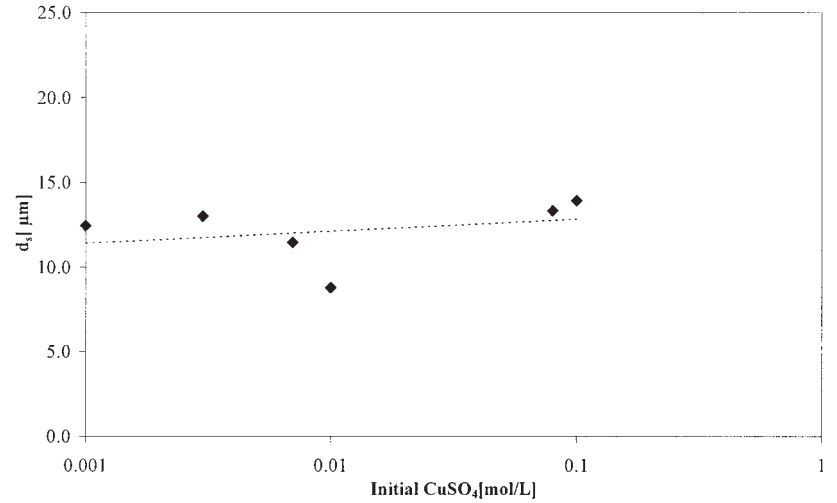

Figure 19. Effect of initial copper ions concentration on the Sautar diameter of the produced particles.

Conditions: $T = 20°C$, $V_L = 1.5$ L, $P = 1.01$ bar, $u_t = 1.41$ cm/s, H_2S gas concentration = 100%.

reactor was studied. First the hydrodynamic behavior of the bubble column reactor was characterized using both CO_2 and H_2S. Then precipitation experiments were carried out. All experiments were performed in the homogeneous regime. Gas holdup and volumetric mass transfer were found to increase with superficial gas velocity in a power-law manner, the exponent being 0.9 for gas holdup and 0.8 for volumetric mass transfer. The highest gas holdup values were obtained when using H_2S gas, whereas volumetric mass transfer was highest when CO_2 was used. The addition of electrolytes led to an increase in the value of the preexponential factor. The presence of ZnS or CuS particles caused enhancement of the H_2S absorption rate, especially at high initial copper- or zinc sulfate concentrations.

Furthermore, it was found that smaller ZnS particles are produced when the H_2S concentration of the gas and/or the $ZnSO_4$ of the solution is increased. No significant effects were observed with copper as a result of severe agglomeration of the surface active CuS particles at the gas–liquid interface. The results of the first part can be used for scale-up purposes. The experimental results were successfully implemented by Paques B.V. in its process design of commercial precipitator. Further study is needed for precise determination of the influences of all relevant process conditions on the average size of the produced solids.

Acknowledgments

This project was supported with a grant of the Dutch Program EET (Economy, Ecology, Technology); a joint initiative of the Ministries of Economic Affairs, Education, Culture and Sciences; and of Housing, Spatial Planning and Environment. This program is coordinated by the EET Program Office, a partnership of Senter and Novem. The authors thank Benno Kaken for his effort in building the experimental setup.

Notation

a = bubble column specific area, m^2/m^3
b = preexponent
c_A^b = bulk concentration of component A in the bubble column, mol/m^3
c_A^o = initial concentration of component A in the bubble column, mol/m^3
$c_{H_2S}^i$ = interfacial concentration of H_2S, mol/m^3
$\bar{c}_{Zn^{2+}}$ = bulk concentration of zinc ions, mol/m^3
D_{col} = diameter of bubble column, cm
D_{H_2S} = diffusion coefficient for H_2S, m^2/s
$D_{Zn^{2+}}$ = diffusion coefficient for zinc ions, m^2/s
E_a = enhancement factor
$E_{A,\infty}$ = infinite enhancement factor
J_{H_2S} = H_2S flux, $mol\ m^{-2}\ s^{-1}$
g = gravitational acceleration, m^2/s
$[H_2S]$ = H_2S concentration, vol %
k_La = volumetric mass transfer coefficient, 1/s
$\dot{m}_{in}$ = inlet mass flow, mol/s
$\dot{m}_{out}$ = outlet mass flow, mol/s
n = exponent
P = pressure, bar
V_d = dispersed volume, m^3
V_L = volume of the liquid in the bubble column, L
u_t = superficial velocity, m/s
T = temperature, °C
t = time, s
X = conversion of metal into metal sulfides, %
ρ_L = liquid density, kg/m^3
ε_G = gas holdup
$\nu_{Zn^{2+}}$ = reaction stoichiometric

Literature Cited

1. Deckwer WD. *Bubble Column Reactors*. London: Wiley; 1992.
2. Joshi JB. Computational flow modeling and design of bubble column reactors. *Chemical Engineering Science.* 2001;56:5893-5933.
3. Eigenberger G, Bauer M. A concept for multi-scale modeling of bubble columns and loop reactors. *Chemical Engineering Science.* 1999;54:5109-5117.
4. Jones AG, Rigopoulos S. Dynamic modeling of bubble column for particle formation via a gas–liquid reaction. *Chemical Engineering Science.* 2001;56:6177-6184.
5. Mersmann A. Batch precipitation of barium carbonate. *Chemical Engineering Science.* 1993;48:3083-3088.
6. Al-Tarazi M, Heesink B, Versteeg G. New method for the determination of precipitation kinetics. Proceedings of 4th Jordanian International Chemical Engineering Conference, Sep. 22–24, Amman, Jordan; 2002.
7. Teixeira JA, Freitas C, Fialova M, Zahradnik J. Hydrodynamics of three-phase external-loop airlift bioreactor. *Chemical Engineering Science*. 2000;55:4961-4972.
8. Paques B.V., Balk, The Netherlands, www.paques.nl.
9. Marracci G. A theory of coalescence. *Chemical Engineering Science.* 1969;24:975-987.
10. Alvarez-Cuena M, Nerenberg MA. The plug flow model for mass transfer in three phase fluidized beds and bubble columns. *Canadian Journal of Chemical Engineering.* 1981;59:739-745.
11. Wach S, Jones AG. Mass transfer with chemical reaction and precipitation. *Chemical Engineering Science.* 1990;40:1027-1033.
12. Tsutsumi A, Nieh J-Y, Fan L-S. Role of the bubble wake in fine particle production of calcium carbonate in bubble column system. *Industrial and Engineering Chemistry.* 1991;30:2328-2333.
13. Jones AJ, Hostomsky J, Li Z. On the effect of liquid mixing rate on primary crystal size during the gas–liquid precipitation of calcium carbonate. *Chemical Engineering Science.* 1992;47:3817-3824.
14. Deckwer WD, Schumple A. Improved tools for bubble column reactor design and scale-up. *Chemical Engineering Science.* 1993;48:889-911.
15. Hostomsky J, Jones AG. A penetration model of the gas–liquid reactive precipitation of calcium carbonate crystals. *Transactions of the Institution of Chemical Engineering.* 1995;73:241-245.
16. Kluytmans JHJ, van Wachem BGM, Kuster BFM, Schouten JC. Gas holdup in a slurry bubble column: Influence of electrolyte and carbon particles. *Industrial and Engineering Chemistry Research.* 2001;40:5326-5333.
17. Bouaifl M, Hebrard G, Bastoul D, Roustan M. A comparative study of gas holdup, bubble size, interfacial area and mass transfer coefficients in stirred gas–liquid reactors and bubble columns. *Chemical and Process Engineering*. 2001;40:97-111.
18. Koide K. Design parameters of bubble column reactors with and without solid suspensions. *Journal of Chemical Engineering of Japan*. 1996;29:5.
19. Christenson HK, Yaminsky V. Solute effects on bubble coalescence. *Journal of Physical Chemistry.* 1995;99:10420.
20. Trambouze P, Van Laneghem H, Wauquier JP. *Chemical Reactors: Design/Engineering/Operation*. Paris, France: Editions TECHNIP; 1988.
21. Versteeg GF, Kuipers JAM, Beckum FPH, Van Swaaij WPM. Mass transfer with complex reversible chemical reactions—I. Single reversible chemical reaction. *Chemical Engineering Science.* 1989;44:2295-2310.

Manuscript received Jan. 27, 2004, and revision received May 20, 2004.